Modelling cluster wakes and wind farm blockage

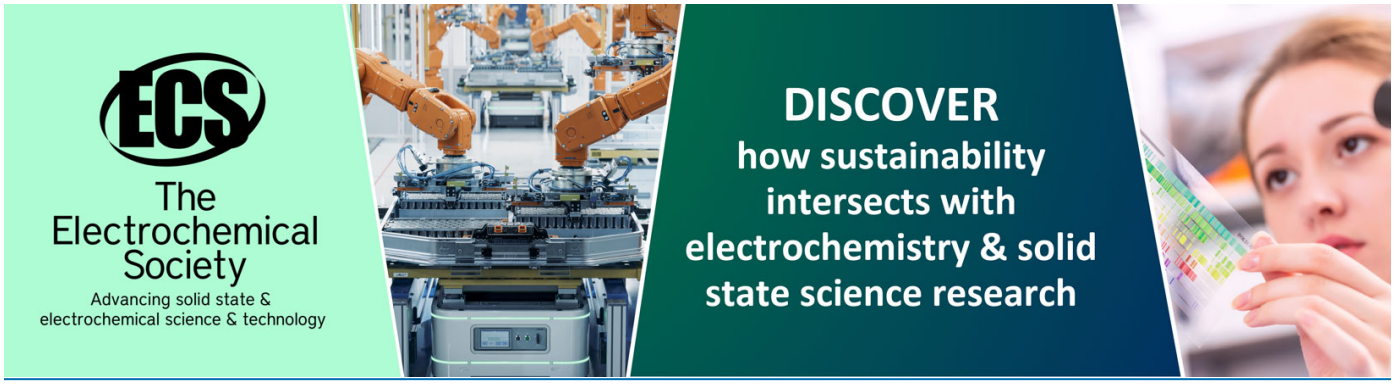

Modelling cluster wakes and wind farm blockage

Nicolai Gayle Nygaard, Søren Trads Steen, Lina Poulsen and Jesper Grønnegaard Pedersen

Ørsted, Kraftværksvej 53, 7000 Fredericia, Denmark

E-mail: nicny@orsted.dk

Abstract. We present two new models for wind turbine interaction effects and a recipe for combining them. The first model is an extension of the Park model, which explicitly incorporates turbulence, both the ambient atmospheric turbulence and the turbulence generated in the wake itself. This Turbulence Optimized Park model is better equipped to describe wake recovery over long distances such as between wind farms, where the wake expansion slows down as the turbine-generated turbulence decays. The second model is a first version of a full engineering wind farm blockage model. In the same vein as the wake model it adds blockage contributions from the individual wind turbines to form an aggregated wind farm scale blockage effect that can be incorporated directly into the park power curve and annual energy calculations. The wake model and the blockage model describe downstream and upstream turbine interaction effects, respectively. They are coupled as the outputs of one model are the inputs to the other model and vice versa. We describe how this coupling is achieved through an iterative process. We give early stage examples of the validation of the two models and discuss how they might be further validated and improved in the future.

1. Introduction

The interaction between wind turbines placed in arrays lead to losses that are crucial to understand and characterize when estimating the energy production of wind farms. However, there is an emerging understanding that some physical aspects of wind turbine interactions have been misrepresented or neglected in industry energy yield calculations, leading to an overestimation bias in the predicted annual energy production.

One source of bias are the wakes between wind farms occurring in clusters consisting of multiple wind farms. The importance of modelling these cluster wakes has long been acknowledged. However, measurements with satellite-based synthetic aperture radar [1, 2, 3, 4], aircraft [2], scanning lidar [3] and dual-Doppler radar [4, 5] have shown that cluster wakes may persist longer than previously assumed. This implies that cluster wakes have a larger impact on the production of downstream wind farms than captured by current engineering wake models [6].

At the same time research has uncovered wind speed reductions upstream of wind farms consistent with a blockage effect induced by the wind farms themselves [7, 8]. Such an upstream effect of the turbines on the flow is not included in the assumptions underlying the wake models typically used to characterize turbine interaction effects. This leads to an overprediction bias in wind farm energy estimates.

The wind speed reduction by a single turbine in its induction zone is well-known in fluid dynamics. The new aspect is the aggregation of these turbine induction effects into a wind farm

scale blockage effect. The wind farm blockage effect leads to variation in the power production of unwaked front row turbines [9] and biases power curve measurements through the wind speed reduction in front of the test turbine [10]. High fidelity simulations show how the interaction of the wind farm with the atmosphere above may aggravate the wind farm blockage effect in stable atmospheric conditions [11, 12].

While there is a growing consensus that the losses due to wakes from neighbouring wind farms and the wind farm blockage effect have hitherto been underestimated or neglected, the engineering tools for simple yet accurate estimation of these effects are missing. In this paper we bridge that gap by introducing two new wind turbine interaction models. The first model extends the Park wake model by coupling the wake expansion to the local turbulence intensity including the turbulence generated in the wake itself. This leads to a slower wake recovery behind the wind farm, where the wake-generated turbulence is decaying with distance. The result is larger cluster wake losses. The second model is an engineering description of the aggregated blockage effect of all the turbines in an array leading to a wind farm blockage effect. An important component is the coupling between the wake model and the blockage model for a coherent description of wind turbine interaction effects.

The two new models and the coupling scheme are introduced in Sections 2, 3 and 4, where we also show the results of preliminary validations. We discuss the implications of the results and possible model improvements and conclude in Section 5.

2. Cluster wakes

In this section, we give a brief review of the Park wake model before deriving a new variation of the model which explicitly accounts for both atmospheric and wake-generated turbulence in the wake expansion. We provide a first validation of this new model, demonstrating that it significantly improves the predictions of cluster wakes.

2.1. The Park wake model

The Park model goes back to Jensen [13] and Kátic *et al.* [14] and is one of several engineering wake models in common use. It specifies the single-turbine wind speed deficit as

$$\delta(x) = 1 - \frac{V(x)}{U_0} = \left(1 - \frac{V_{\text{in}}}{U_0}\sqrt{(1 - C_T(V_{\text{in}})}\right)\left[\frac{D}{D_w(x)}\right]^2 \tag{1}$$

Here $V(x)$ is the wind speed in the wake a distance x downstream of the turbine[1]. In the Park model, $V(x)$ is constant inside the wake cone of diameter $D_w(x)$, resulting in a top-hat cross-stream profile of the wind speed. The rotor diameter of the wake-generating turbine is D. The rotor-averaged inflow wind speed at the turbine position is V_{in}. Importantly, it is reduced relative to the freestream wind speed U_0 due to the wakes from any upstream wind turbines and the induced blockage from lateral and downstream neighbours (see Section 4).

The wind speed deficits from multiple upstream turbines are added in quadrature following the Kátic *et al.* superposition rule [14]. Note that all the individual deficits are calculated relative to the freestream wind speed U_0. The effect of the ground surface is simulated using image turbines below the surface [15]. If a turbine is stopped, its deficit is set to zero.

As the wake propagates downstream, the diameter of the wake increases. This in turn reduces the wind speed deficit. Asymptotically, the wind speed recovers to the freestream value. In the Park model the wake expansion is linear:

$$D_w(x) = D + 2kx \tag{2}$$

[1] Throughout this paper we adopt a model coordinate system where the positive x-axis is aligned with the wind direction. For a turbine placed at the origin, x is positive downstream and negative upstream of the rotor.

The single tunable parameter of the model is the wake decay constant k. For offshore wind farms, a value between 0.03 and 0.05 is recommended [16, 17, 18]. The Park model has been demonstrated to give a good description of interior wake losses in both offshore [18] and onshore wind farms [19] as well as the wakes from nearby neighbouring wind farms (within 3 km) [20]. In section 2.3, we show by example that this predictive accuracy does not extend to the wakes between wind farms separated by larger distances.

2.2. The Turbulence Optimized Park model

Physically, the wake expansion rate is linked with the amount of turbulence, with increased turbulent mixing leading to a faster wake expansion and wind speed recovery [17]. A correlation between the atmospheric turbulence intensity and the wake losses in wind farms has been pointed out by several authors, e.g. [18] and [21]. The Park model wake decay constant has thus been related to the turbulence intensity at hub height [19].

Besides the ambient turbulence in the atmosphere the wake expansion is affected by the additional turbulence in the wake generated by shear on the wake edge. Niayifar and Porté-Agel have proposed a wind farm model, where the wake expansion is driven by the inflow turbulence intensity, which is the combination of the ambient turbulence and the turbulence generated by the upstream turbines [22]. This concept has been tested against field data in [23].

We propose that the wake expansion remains locally linear, with an expansion rate determined by the local turbulence intensity $I(x)$ in the wake and a model calibration constant A:

$$\frac{dD_w}{dx} = AI(x) \tag{3}$$

The concept of a wake growth rate proportional to the combination of atmospheric and wake generated turbulence goes back to Lissaman [15]. It is also related to the concept behind eddy-viscosity models [24]. The novel result presented here is the analytical integration of that expansion rate for a particular wake-added turbulence model.

Several different models exist for the combination of the background atmospheric turbulence intensity I_0 with the additional turbulence $I_w(x)$ generated in the wake. Here we use the Frandsen wake turbulence model [25], which is utilized for loads calculations in the IEC 61400-1 edition 3 standard [26] and has been validated against turbulence measurements in offshore wind farms [27]. In the Frandsen model, the two sources of turbulence are added in quadrature

$$I(x) = \sqrt{I_0^2 + I_w^2(x)} \tag{4}$$

The additional turbulence in the wake is described empirically as

$$I_w(x) = \frac{1}{c_1 + c_2 \frac{x/D}{\sqrt{C_T(V_{\text{in}})}}} \tag{5}$$

The two constants $c_1 = 1.5$ and $c_2 = 0.8$ are given in [26]. The combined turbulence intensity asymptotically approaches the ambient atmospheric turbulence intensity with increasing downstream distance. Hence the wake expansion is fastest closest to the turbine, where the wake contribution to the turbulence is largest. Further downstream the wake expansion slows down, asymptotically reaching a linear expansion at a constant rate rate.

To find the wake diameter at a specific downstream distance the turbulence-dependent local expansion rate can be integrated from the rotor location ($x = 0$ in our coordinate system),

where the wake width is assumed to equal the rotor diameter, to x. The definite integral has the analytical solution

$$D_w(x) = D + \frac{AI_0D}{\beta}\left(\sqrt{(\alpha+\beta x/D)^2+1} - \sqrt{1+\alpha^2} - \ln\left[\frac{\left(\sqrt{(\alpha+\beta x/D)^2+1}+1\right)\alpha}{(\sqrt{1+\alpha^2}+1)(\alpha+\beta x/D)}\right]\right) \quad (6)$$

We have introduced the auxiliary variables $\alpha = c_1 I_0$ and $\beta = c_2 I_0/\sqrt{C_T(V_{\text{in}})}$. Both α and β are positive. Together with the wind speed deficit equation (1) the non-linear wake expansion expression constitutes the Turbulence Optimized Park model (TurbOPark). As in the original Park model, overlapping wakes are added in quadrature. Based on a preliminary calibration on a subset of Ørsted's offshore wind farms the recommended value of the expansion parameter is $A = 0.6$. This recommendation is subject to change when the validation is repeated on a wider data set.

Figure 1 compares the wake expansion in the Park and TurbOPark models. In the TurbOPark model, the wake expansion and hence recovery slows down significantly with increasing distance behind the turbine, as the turbulence generated by the rotor dissipates, and the mixing process becomes dominated by the background atmospheric turbulence. Consequently, the wakes persist longer and lead to larger losses for downstream turbines and wind farms than in the traditional Park model.

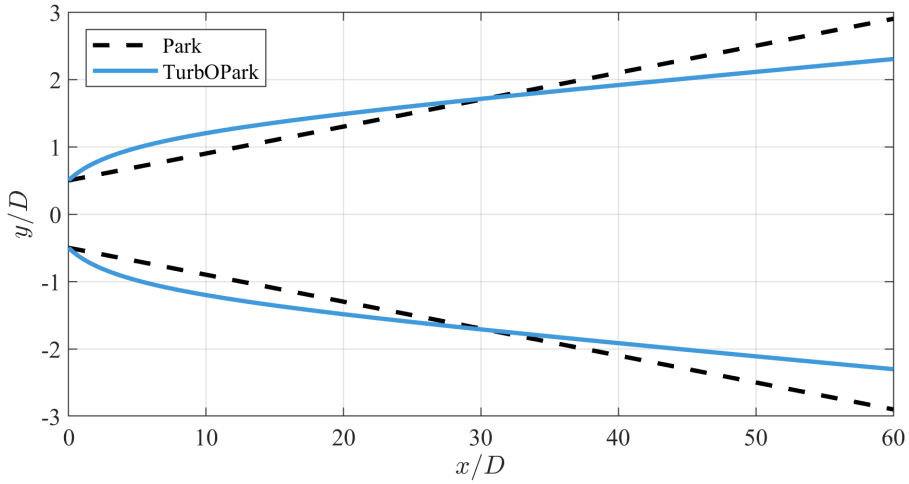

Figure 1. Illustration of wake expansion in the Park model with $k = 0.04$ (dashed black line) and the TurbOPark model with $A = 0.6$ and ambient turbulence $I_0 = 6\%$ (blue solid line).

2.3. Validation with wind farm data

In a first validation the new TurbOPark model is compared with the Park model and with operational wind farm data from the Supervisory Control and Data Acquisition (SCADA) system. The offshore wind farm is Westermost Rough, which is located off the Yorkshire coast in the UK. It consists of 35 Siemens 6 MW turbines with a hub height of 102 m above mean sea level and a 154 m rotor diameter. The layout is shown in Figure 2 (inset). The wind speeds predicted by the wake models at the turbine positions are converted to power using the power curve from the turbine manufacturer.

For the ambient turbulence intensity we use (non-concurrent) measurements from the Humber Gateway met mast, suitably corrected for mast shadow effects. At 8 m/s, the mean ambient turbulence intensity was determined to be 5.9% at 90 m above mean sea level.

We first compare the model outputs with the observed power variation along a row of turbines, Figure 2. The power of every turbine is normalized by the power of the front turbine in the row. Data are filtered on a 30° wind direction sector aligned with the row (wind from the northwest) and a wind speed at the front turbine of 8 ± 0.5 m/s. Furthermore, we require that all turbines in the row as well as turbines with a wake impacting the row are operating normally. The model predictions are calculated in one-degree wind direction increments and averaged over the inflow sector weighted by the distribution of wind directions in the data.

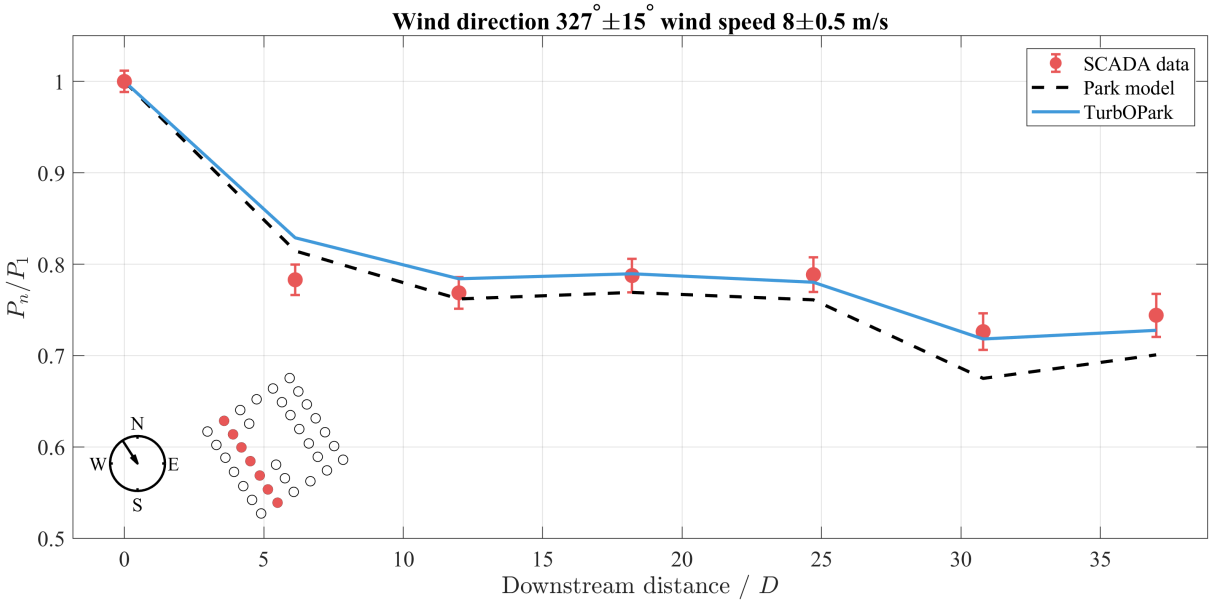

Figure 2. Relative power along a row of turbines in Westermost Rough (red circles). The error bars represent the 95% confidence interval for the mean. The row and the wind direction are indicated in the inset. Outputs from TurbOPark with ambient turbulence $I_0 = 5.9\%$ (blue line) and the Park model with $k = 0.04$ (dashed line) are plotted for the same range of inflow conditions.

The predicted power of the TurbOPark model is close to the results from the Park model and both match the observations reasonably. A similar agreement is found for other turbine rows (not shown). This gives confidence that the TurbOPark model prediction of internal wind farm wakes is at least as good as those of the Park model. The calibration of the wake expansion parameter A did not include any data from Westermost Rough to ensure independence of the validation presented here.

In contrast with the model performance for internal wakes, the quality of the two models show a stark difference for cluster wakes as illustrated in Figure 3, where we investigate the influence of the Humber Gateway wind farm on Westermost Rough. Humber Gateway is located 15 km to the southeast of Westermost Rough, see Figure 3(b,c). It is made up of 73 Vestas 3 MW turbines with a rotor span of 112 m and a hub height of 80 m. We do not have access to SCADA data from Humber Gateway. Therefore, the freestream wind speed to be input to the wake models must be estimated from Westermost Rough data. Furthermore, to separate

the effect of cluster wakes from the internal wakes we focus on two two corner turbines in the front row, labelled A01 and F01 in Figure 3. For wind directions between 135° and 155° turbine A01 is in the wake from Humber Gateway, while F01 is unwaked. As the wind direction increases, A01 escapes the wake from the upstream neighbour wind farm, which instead moves over F01. For wind directions exceeding 175° F01 is also free off the cluster wake. The sweeping of the wake from Humber Gateway across Westermost Rough with changing wind direction leads to a characteristic sinusoidal variation of the power ratio between the two corner turbines, Figure 3(a). We use the maximum wind speed among the two turbines as an indication of the freestream wind speed. We only include situations where both A01 and F01 are running normally and where the estimated freestream wind speed is between 7.5 m/s and 8.5 m/s. The observations are averaged in 5° wind direction sectors.

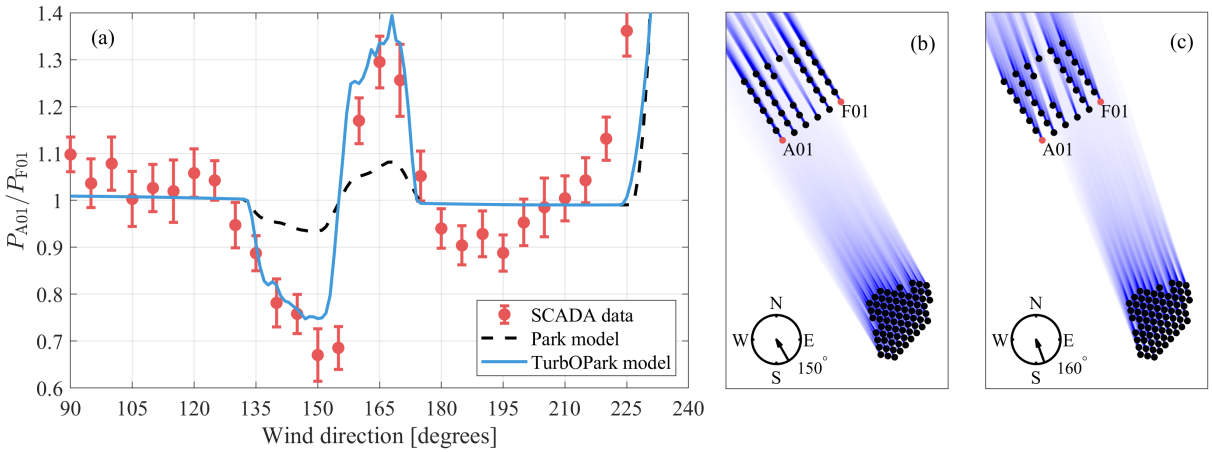

Figure 3. (a): the power ratio of the Westermost Rough corner turbines A01 and F01 as a function of the wind direction. The inflow wind speed is 8 ± 0.5 m/s (see text). The SCADA data are averaged in 5° sectors (red circles) with error bars indicating the 95% confidence interval for the mean. Lines are the corresponding Park and TurbOPark ($I_0 = 5.9\%$) model results. (b) and (c): wind farm layouts with Park model wind speed deficits for 150° and 160°, respectively.

Perhaps surprisingly, the wake impact on the front row turbines is 30% in spite of the 15 km separation between the wind farms. The Park model correctly predicts the trend of the sinusoidal variation, but completely fails to capture the magnitude. It underestimates the wake loss from the cluster wakes by more than 20% in this example. In contrast, the TurbOPark model with the site-specific ambient turbulence intensity predicts the correct size of the power deficit. This shows that while the wake expansion rate in the Park model is appropriate for internal wind farm wakes, it is too fast for the wake behind a wind farm, where the turbulent mixing is only driven by the ambient turbulence. This is not unexpected, since the Park model and other engineering wake models have been predominantly calibrated on internal wakes data.

The large increase in the power ratio above 210° is due to internal wakes on F01. We believe that the minimum in the power ratio between 180° and 205° is caused by coastal wind speed gradients that lead to an increase of the wind speed from A01 to F01 in those directions.

3. Wind farm blockage

We build a simple wind farm blockage model on the accumulation of single-turbine induction effects described by a vortex cylinder model. In the vortex cylinder model [28, 29], the induced axial velocity is axisymmetric about the center of the rotor, depending only on the streamwise

position x, the radial distance $r = \sqrt{y^2 + z^2}$ from the rotor centre[2] and vorticity γ:

$$u(x,r) = \frac{\gamma}{2}\left(\frac{R - r + |R - r|}{2|R - r|} + \frac{xm(x,r)}{2\pi\sqrt{rR}}\left[K\left(m(x,r)\right) + \frac{R-r}{R+r}\Pi\left(m(0,r), m(x,r)\right)\right]\right) \tag{7}$$

where K and Π are the complete elliptic integrals of the first and third kind, respectively. The parameter m depends only on the position relative to the rotor and the rotor radius $R = D/2$:

$$m^2(x,r) = \frac{4rR}{x^2 + (R+r)^2} \tag{8}$$

We assume that there is no yaw misalignment, such that the axial and streamwise velocity components are equal. For notational simplicity we introduce a geometric factor $F(x,y,z)$ and write the induced velocity as $u(x,y,z|\gamma) = \gamma F(x,y,z)/2$. The geometric factor describes the spatial variation of the induced axial velocity.

On the rotor plane ($x = 0$), the induced velocity is constant and equal to $\gamma/2$ for $r < R$ and zero otherwise [28]. This enables the establishment of a relation between the vortex strength γ and the thrust of the turbine through 1D momentum theory. The latter specifies that the wind speed at the rotor disk is $U_0(1-a)$, where $a = \frac{1}{2}[1 - \sqrt{1 - C_T(V_{\text{in}})}]$ is the axial induction factor. Equating the wind speed reduction at the rotor to $u(0, r < R)$ the vorticity is found to be

$$\gamma = -2aU_0 = -U_0\left[1 - \sqrt{1 - C_T(V_{\text{in}})}\right] \tag{9}$$

Note that this depends on the local inflow wind speed to the rotor V_{in} through the thrust coefficient. This becomes important, when the turbine is operating in wake conditions.

The vortex cylinder model describes an actuator disk in uniform inflow. To simulate the effect of the ground surface we use an image rotor at $(0, 0, -2z_H)$ in the coordinate system centered on the rotor. The total wind speed blockage effect from a turbine is then

$$\tilde{u}(x,y,z|\gamma) = \frac{\gamma}{2}\left[F(x,y,z) + F(x,y,z+2z_H)\right] \tag{10}$$

In this first version of the wind farm blockage model, we neglect the acceleration of the flow around the rotor by setting $\tilde{u}(x > 0, y, z) = 0$. The intention is to let the wake model describe all downstream developments of the flow, while the blockage model handles the upstream region.

To build a wind farm blockage model we use the induced velocities from the individual turbines as building blocks. Since the induction effects from multiple vortex cylinders are additive, the aggregated blockage induced wind speed change at turbine i can be written as a sum over all N turbines with vorticities γ_j:

$$\Delta U_i = \sum_{j=1}^{N} \tilde{u}(x_i - x_j, y_i - y_j, z_{H,i} - z_{H,j}|\gamma_j) + a_i U_0 \tag{11}$$

The last term is a correction to avoid double counting the self-induction from the turbine, which is already accounted for (at least partially) in the power and thrust curves[3]. The coordinates are in the frame, where the positive x axis is aligned with the wind direction. Hence the blockage effect must be recalculated for each wind direction. As $\Delta U_i < 0$, the wind speed at a turbine

[2] The origin of our coordinate system is at the rotor centre. With this convention the ground surface is at $z = -z_H$, where z_H is the hub height.

[3] We do include the blockage effect from the image turbine at position i, since it is our understanding that this is not explicitly accounted for in the power and thrust curves provided by turbine manufacturers.

is reduced relative to the freestream due to the blockage effect of the turbines behind it. This leads to a loss in the calculation of the wind farm energy yield.

Gribben and Hawkes propose that the vortex cylinder can be replaced with a Rankine Half Body, which is computationally more efficient, since the model is analytical and no numerical evaluations of the complete elliptic integrals are needed [30]. Away from the rotor the flow patterns of this potential flow model are nearly identical to those of the vortex cylinder.

4. Coupling wind farm blockage with wakes

The blockage model needs the thrust coefficient of every turbine as inputs. These are outputs from the wake model, as turbines operating in wake experience a lower inflow wind speed, leading to a modified C_T. Conversely, the blockage from the other turbines in the wind farm changes the available wind speed at every turbine position. This necessitates a coupling between the wake model and the wind farm blockage model, whereby the output from one model forms part of the inputs for the other and vice versa. We solve this problem iteratively for each wind speed and wind direction combination:

(i) The wake model is solved in the upwind to downwind direction. This results in turbine-specific C_T values reflecting the pattern of the wake-induced wind speed variation

(ii) The wind farm blockage effect at each turbine position is calculated in the downwind to upwind direction using the C_T values returned in step (i) as inputs. This reduces the wind speed at each turbine position in the absence of wakes from U_0 to $U_{0i} = U_0(1 + \Delta U_i/U_0)$

(iii) The wake model is run again with U_{0i} replacing U_0

Steps (ii) and (iii) should be repeated until the wind speeds at each turbine has converged. Experiments show that the scheme converges very quickly. In practice it is only necessary to run through steps (i)-(iii) once.

This iterative framework is independent of the specifics of both the wake and the blockage model implementations. The only requirement is that both models are based on the superposition of wind turbine interaction effects from individual turbines. Hence it is possible to replace the wake and/or the blockage model used here with another model.

4.1. Validation with wind farm data

At this point, an extensive validation of the coupled wakes and blockage wind farm model has not been undertaken. However, two examples are shown in Figures 4 and 5. To isolate the blockage part of the model we focus on the front row turbines that are unaffected by wakes. The examples compare the model outputs with SCADA data from the wind farm Gunfleet Sands in the Thames estuary in the UK. It is a regular grid of 48 Siemens 3.6 MW turbines with a rotor diameter of 107 m. The hub height is 77.5 m above mean sea level.

We choose one turbine (labelled 1 in Figures 4 and 5) as the reference and normalize the power of the other front row turbine to that. Data are filtered on wind direction and the wind speed at the reference turbine. We only include data where all the front row turbines and at least 90% of all turbines are operating normally. Without access to the freestream wind speed, we run the model at multiple inflow wind speeds and choose the results where the modelled wind speed at the reference turbine is closest to 8 m/s. Results spanning the sector are averaged.

For a wind direction of 110°, the predicted pattern of power variation across the front row matches the observations reasonably with a tendency for the model to underestimate the variation due to blockage, Figure 4. For a direction of 80°, where the wind is at a more acute angle with the front row, the discrepancy is larger. This shows that in its present form the model is likely missing some element of the relevant physics.

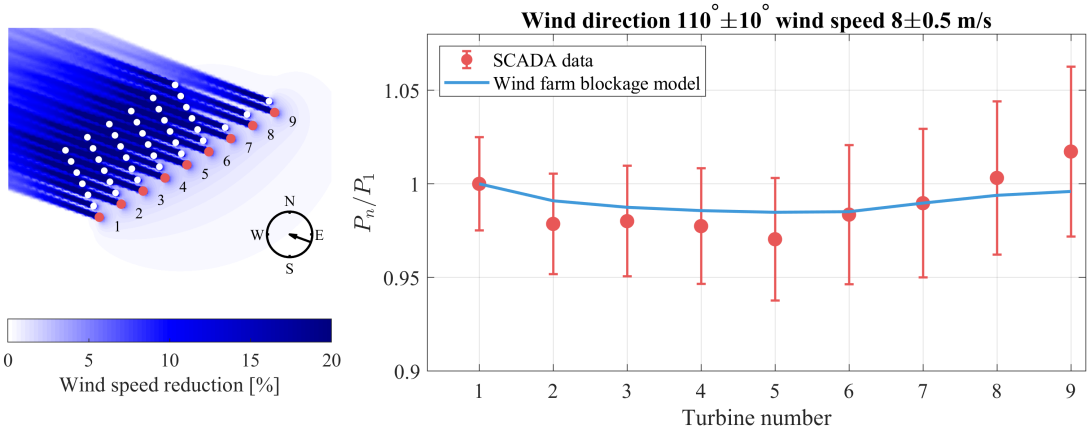

Figure 4. The wind speed deficit in the combined blockage and wakes model (left). The power of the front row turbines normalized to turbine 1 (right). The SCADA data are plotted with red circles, where the error bars represent the 95% confidence interval for the mean. The result of the wind farm blockage model is shown with the blue line.

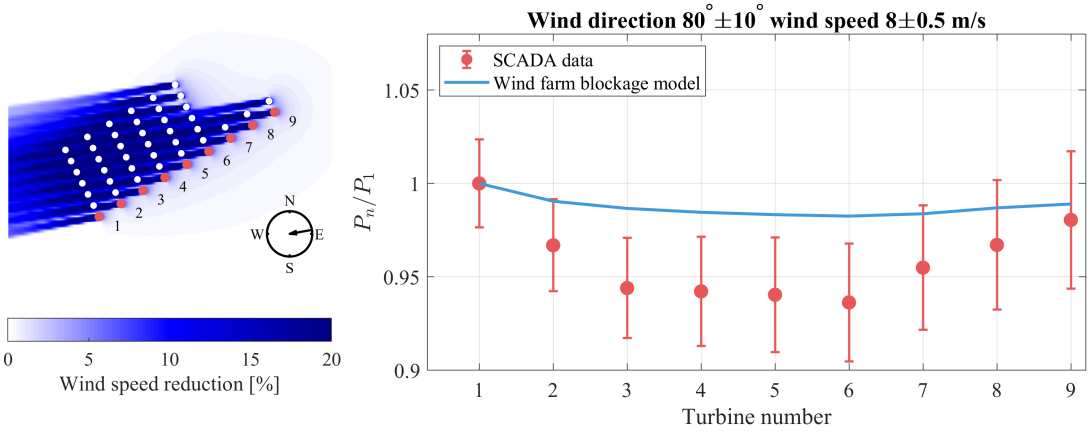

Figure 5. Same as 4 but for a different wind direction.

5. Conclusion

We have described how cluster wakes and wind farm blockage lead to increased turbine interaction losses in wind farms. If these effects are underestimated or neglected it leads to overestimation bias in the production estimate. The size of the bias will depend on the site-specific layout and wind conditions. We have taken steps to minimize this bias by introducing the TurbOPark wake model and a wind farm blockage model as well as a recipe for coupling wakes and blockage in a combined wind turbine interaction model. Initial validations of these models against operational wind farm data demonstrate that TurbOPark captures cluster wakes much better than the Park model. The wind farm blockage model predicts the trend in the variation of power among front row turbines while underestimating its amplitude.

It is clear that more research is needed to ensure that the models are correctly calibrated and include the relevant physics. Further work will focus primarily on additional validation of both models. However, several model improvements are possible. The TurbOPark model may be straightforwardly extended from a top-hat to a Gaussian wind speed profile as in [22]. Likewise, the turbulence influence of upstream turbines may be included. It will also be explored, if a linear wake superposition (consistent with the addition of individual blockage contributions)

is preferable. Any such model modification would require a re-calibration of the expansion parameter. The present wind farm blockage model is a very simple superposition of turbine induction effects. It does not satisfy mass conservation at the wind farm level and neglects the interaction of the wind farm with the atmospheric boundary layer above it. It has been suggested by high fidelity simulations that feedback between the boundary layer and the wind farm may significantly enhance the blockage effect in some circumstances [11, 12]. In further development of the wind farm blockage model, the acceleration of the flow around the rotor may also be incorporated. We note that this would require a re-calibration of the wake model due to the modification of the downstream flow from the induction model.

Engineering models of wind turbine interaction effects like the ones described here remain essential tools in energy yield calculations, since they facilitate rapid assessment of multiple scenarios and can be easily incorporated into the optimization of the wind farm design.

Acknowledgments

We thank Emmanuel Branlard for insightful discussions about rotor and wind farm induction effects.

References

[1] Bay Hasager C, Vincent P, Badger J, Badger M, Di Bella A, Peña A, Husson R and Volker P J H 2015 *Energies* **8** 5413
[2] Platis A, Siedersleben S, Bange J *et al.* 2018 *Sci. Rep.* **8** 2163
[3] Schneemann J, Rott A, Dörenkämper M, Steinfeld G and Kühn, M 2020 *Wind Energy Science* **5** 29
[4] Ahsbahs T, Nygaard N G, Newcombe A, Badger M 2020 *Remote Sens.* **12** 462
[5] Nygaard N G, Newcombe A C 2018 *J. Phys.: Conf. Ser.* **1037** 072008
[6] Cañadillas B, Foreman R, Barth V, *et al.* 2020 *Wind Energy* **23** 1249
[7] Bleeg J, Purcell M, Ruisi R and Traiger E 2018 *Energies* **11** 1609
[8] Segalini A and Dahlberg J-Å 2020 *Wind Energy* **23** 120
[9] Mitraszewski K, Hansen K S, Nygaard N G and Rethoré P E 2012 *Science of Making Torque from Wind conference* Oldenburg Germany
[10] Nygaard N G and Ettrup Brink F 2017 *Wind Energy Science Conference* Lyngby Denmark
[11] Wu K L and Porté-Agel F 2017 *Energies* **10** 2164
[12] Allaerts D, Vanden Broucke S, van Lipzig N and Meyers J 2018 *J. Phys.: Conf. Ser.* **1037** 072006
[13] Jensen N O 1983 *A Note on Wind Generator Interaction* Risø report M-2411 (Roskilde, Denmark)
[14] Kátic I, Højstrup J and Jensen N O 1986 *Proc. Eur. Wind Energy Conf.* (Rome)
[15] Lissaman P B S and Bate Jr E R 1977 *Energy Effectiveness of Arrays of Wind Energy Conversion Systems* AeroVironment Inc. (Pasadena, California) AV-FR-7058
[16] Barthelmie R J and Jensen L E 2010 *Wind Energy* **13** 573
[17] Porté-Agel F, Bastankhah M and Shamsoddin S 2019 *Boundary-Layer Meteorol* **174** 1
[18] Nygaard N G 2014 *J. Phys.: Conf. Ser.* **524** 012612
[19] Peña A, Réthoré P-E and van der Laan M P 2016 *Wind Energy* **19** 763
[20] Nygaard N G and Hansen S D 2016 *J. Phys.: Conf. Ser.* **753** 032020
[21] Hansen K S, Barthelmie R J, Jensen L E and Sommer A 2012 *Wind Energy* **15** 183
[22] Niayifar A and Porté-Agel F 2015 *J. Phys.: Conf. Ser.* **625** 012039
[23] Duc T, Coupiac O, Girard N, Giebel G and Göçmen T 2019 *Wind Energy Science* **4** 287
[24] Ainslie J F 1988 *J. Wind Eng. Ind. Aerodyn.* **27** 213
[25] Frandsen S 2003 *Turbulence and turbulence generated structural loading in wind turbine clusters* Risø report R-1188 (Roskilde, Denmark)
[26] IEC Standard, 61400–1, Edition 3 + amendment 1, 2010
[27] Argyle P, Watson S, Montavon C, Jones I and Smith M 2018 *Wind Energy* **21** 1329
[28] Branlard E 2017 *Wind Turbine Aerodynamics and Vorticity-Based Methods: Fundamentals and Recent Applications* (Berlin, Germany: Springer)
[29] Branlard E and Meyer Forsting A R 2019 *Wind Energy* submitted
[30] Gribben B J and Hawkes G S 2019 *A potential flow model for wind turbine induction and wind farm blockage* Frazer-Nash Technical Paper